Biology of Reproduction, 2020, 103(5), 986–999
doi:10.1093/biolre/ioaa139
Research Article
Advance Access Publication Date: 6 August 2020

OXFORD

Research Article

Age-related alterations in fertilization-induced Ca^{2+} oscillations depend on the genetic background of mouse oocytes†

Katarzyna Czajkowska[1], Agnieszka Walewska[1], Takao Ishikawa[2], Katarzyna Szczepańska[1] and Anna Ajduk[1,*]

[1]Department of Embryology, Faculty of Biology, University of Warsaw, Warsaw, Poland and [2]Department of Molecular Biology, Faculty of Biology, University of Warsaw, Warsaw, Poland

***Correspondence:** Department of Embryology, Faculty of Biology, University of Warsaw, Warsaw, Poland.
Tel.: +48-22-5541212, Fax.: +48-22-5541210, E-mail: aajduk@biol.uw.edu.pl

†Grant Support: The project was founded by the Sonata grant (UMO-2012/07/D/NZ5/04301) from the National Science Centre (Poland) to AA.

Received 1 August 2020; Revised 5 June 2020; Editorial Decision 3 August 2020; Accepted 8 August 2020

Abstract

Maternal aging affects various aspects of oocytes' physiology, including the functionality of their nuclear apparatus and mitochondria. In the present paper, we wished to investigate whether advanced reproductive age impacts oocytes' ability to generate proper Ca^{2+} oscillations in response to monospermic fertilization. We examined three different mouse strains/crosses: inbred C57BL/6Tar, outbred Tar:SWISS, and hybrid F1 (C57BL/6Tar × CBA/Tar). The females were either 2–4 months old (young) or 13–16 months old (aged). We observed that the Ca^{2+} oscillatory pattern is altered in a strain-dependent manner and changes were more profound in aged C57BL/6Tar and F1 than in aged Tar:SWISS oocytes. We also showed that maternal aging differently affects the size of Ca^{2+} store and expression of *Itpr1*, *Atp2a2*, *Erp44*, and *Pdia3* genes involved in Ca^{2+} homeostasis in oocytes of C57BL/6Tar, Tar:SWISS, and F1 genetic background, which may explain partially the differences in the extent of age-dependent changes in the Ca^{2+} oscillations in those oocytes. Maternal aging did not have any visible impact on the distribution of the ER cisterns in oocytes of all three genetic types. Finally, we showed that maternal aging alters the timing of the first embryonic interphase onset and that this timing correlates in C57BL/6Tar and Tar:SWISS oocytes with the frequency of fertilization-induced Ca^{2+} oscillations. Our results indicate that extreme caution is required when conclusions about oocyte/embryo physiological response to aging are made and complement an increasing amount of evidence that mammalian (including human) susceptibility to aging differs greatly depending on the genetic background of the individual.

Summary Sentence

The impact of maternal aging on Ca^{2+} homeostasis in fertilized mouse oocytes varies depending on the genetic origin of females.

Graphical Abstract

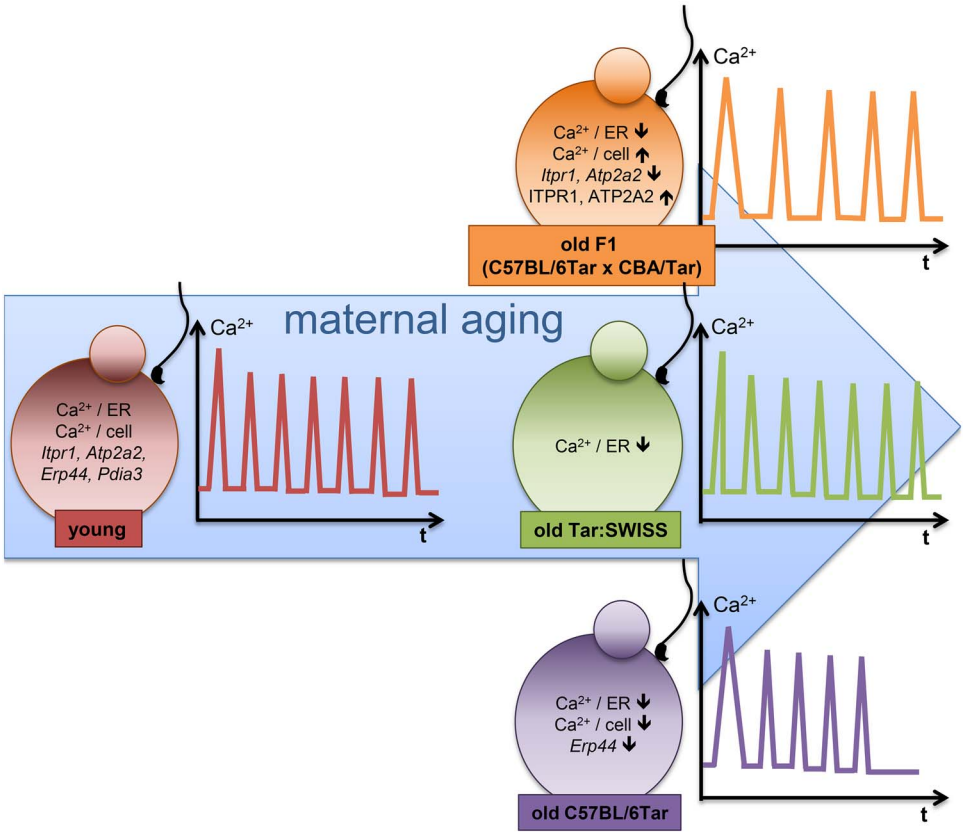

Key words: aging, calcium, fertilization, oocyte.

Introduction

Maternal aging involves changes occurring gradually in oocytes during a female's life, which become particularly pronounced when the female achieves an advanced reproductive age. During maternal aging, the quality of oocytes decreases, which leads to the reduced developmental potential of the resulting embryos (e.g., fragmentation of cleaving embryos, increased apoptosis in blastocysts, and implantation failure) and contributes to reduced fertility of aged females, including women over 35 years of age (reviewed in [1]). Advanced reproductive age coincides in oocytes with altered gene expression on both mRNA and protein levels, including genes regulating the function of nuclear apparatus and mitochondria [2–6]. This leads to aneuploidy and defective energy metabolism often observed in oocytes obtained from older females (reviewed in [7, 8]).

In the present paper, we wished to investigate whether maternal aging also influences the mechanism regulating Ca^{2+} homeostasis in mammalian oocytes and, as a consequence, the course of the sperm-induced Ca^{2+} oscillations. This question is particularly important in the context of oocyte/embryo quality because Ca^{2+} oscillations are an important trigger, mediator, and regulator of numerous processes occurring at the onset of embryonic development. Initiation of each of these processes requires that cytoplasmic concentration of free Ca^{2+} ions is raised for a sufficiently long time, i.e., that there is an adequate number of Ca^{2+} transients. A single Ca^{2+} burst is sufficient for a mouse oocyte to resume the 2nd meiotic division, but longer Ca^{2+} oscillations are needed for its correct completion and initiation of the 1st embryonic interphase. Repeated Ca^{2+} transients are also necessary to establish the block against polyspermy and initiate the recruitment of maternal mRNAs and synthesis of new proteins required to activate the embryonic genome [9–12].

Ca^{2+} oscillations are triggered by phospholipase C zeta introduced into the oocyte by a sperm [13]. The enzyme hydrolyzes phosphatidylinositol 4,5-bisphosphate (PIP_2) to diacylglycerol (DAG) and inositol 1,4,5-triphosphate (IP_3). IP_3 attaches to its receptors acting as Ca^{2+} channels and located in the endoplasmic reticulum (ER) membrane. In mammalian cells, there are three different isoforms of the IP_3 receptor; however, in oocytes, IP_3 receptor type 1 (ITPR1) is predominantly expressed [14]. The binding of IP_3 to the ITPR1 opens the Ca^{2+} channel and releases Ca^{2+} ions from the ER lumen into the cytoplasm. When the cytoplasmic concentration of Ca^{2+} ions rises above a threshold level, ITPR1 is inhibited, and ATP-dependent Ca^{2+} pump (ATP2A2, also known as SERCA2) is activated, which initiates the uptake of Ca^{2+} ions from the cytoplasm back to the ER. When the cytoplasmic concentration of Ca^{2+} ions decreases, ATP2A2 is inhibited, ITPR1 becomes reactivated, and Ca^{2+} ions are again released from ER into the cytoplasm (reviewed in [15]). These consecutive events of ITPR1-mediated Ca^{2+} release from the ER and ATP2A2-mediated Ca^{2+} uptake to the ER form Ca^{2+} oscillations lasting in mammalian oocytes for several hours, usually until the onset of the first embryonic interphase [16–18].

The impact of maternal aging on mechanisms regulating Ca^{2+} oscillations in fertilized oocytes is not thoroughly examined. The

only report directly addressing this issue, authored by Haverfield and co-workers [19], has shown that in CD1 mouse oocytes, maternal aging does not affect the amount of Ca^{2+} stored in the ER and the pattern of sperm-induced Ca^{2+} oscillations: duration, number, and amplitude of Ca^{2+} transients generated in response to sperm were the same in oocytes from aged and young females. However, aged oocytes displayed less frequent and shorter Ca^{2+} oscillations in response to parthenogenetic activation with $SrCl_2$ solution than oocytes from young females. As dynamics of cellular processes in mouse oocytes/embryos and cell susceptibility to environmental conditions depend on the genetic background [20–30], we wished to investigate whether the lack of significant effect of maternal aging on sperm-induced Ca^{2+} oscillations in oocytes is a universal feature or whether it depends on the mouse strain. We showed that maternal aging alters the pattern of Ca^{2+} oscillations in oocytes obtained from inbred C57BL/6Tar (hereafter called C57BL/6) and hybrid F1 (C57BL/6Tar × CBA/Tar) mice much more profoundly than in oocytes from outbred Tar:SWISS mice (hereafter called SWISS). We also revealed that maternal aging differently affects the amount of Ca^{2+} stored in the oocytes and expression of genes involved in the regulation of the Ca^{2+} oscillations in those mouse types. Finally, we showed that maternal aging alters the timing of the 1st embryonic interphase onset and that this timing correlates with the frequency of Ca^{2+} oscillations in fertilized oocytes of C57BL/6 and SWISS background. Our results indicate that the extreme caution is required when conclusions about oocyte/embryo physiological response to aging, and most likely other environmental conditions as well, are made. Observations presented in this paper complement well an increasing amount of evidence that human physiology and its susceptibility to aging differ greatly depending on the genetic background of the individual (reviewed in [31, 32]).

Materials and methods

Ethics Statement

All experiments were approved by the Local Ethics Committee for Experimentation on Animals no. 1 (Warsaw, Poland) and were performed in compliance with the national regulations.

Animals and reagents

Young (2–4 months old) and old (13–16 months old) outbred Tar:SWISS (SWISS), inbred C57BL/6Tar (C57BL/6), and hybrid F1 (C57BL/6Tar × CBA/Tar) mouse females and hybrid F1 (C57BL/6Tar × CBA/Tar) mouse males (4–6 months old) were maintained in the Animal Facility of the Faculty of Biology, University of Warsaw at 14:10 light/dark cycle and provided with food (standard chow diet; Labofeed H Standard (Wytwórnia Pasz "Morawski", Poland)) and water ad libitum. Males and females were kept in the same room, in open cages with at least 60–100 cm^2 of cage space per mouse, depending on the mouse weight. C57BL/6Tar inbred substrain was derived from B6J substrain and CBA/Tar—from CBA/W substrain; both were bred separately for 20 generations. Old C57BL/6 females were used before the experiments as breeders. Animals were sacrificed by cervical dislocation. All reagents were purchased from Sigma-Aldrich Merck unless stated otherwise.

Oocyte collection

To obtain GV oocytes (i.e., oocytes in prophase of the 1st meiotic division), female mice were primed with an intraperitoneal injection of 10 IU of pregnant mare serum gonadotrophin (PMSG, Intervet). GV oocytes were isolated 48 h later from ovaries into M2 medium (M16 buffered with Hepes [33]) and cultured for 16 h (in vitro maturation) in M16 medium. To obtain ovulated oocytes (in metaphase of the 2nd meiotic division, MII), the PMSG injections were followed 48 h later by 10 IU of human chorionic gonadotrophin (hCG, Intervet). Ovulated oocytes were recovered from oviducts 15 h after hCG and placed in hyaluronidase solution (150 IU/ml in phosphate-buffered saline, PBS) to remove the cumulus cells. Denuded oocytes were washed in M2 medium.

Sperm collection

Epididymal sperm for all experiments involving in vitro fertilization was isolated from F1 males and capacitated in 0.5 mL of fertilization medium with 5 mg/ml bovine serum albumin (BSA) [34] for 1.5–2 h in 37.5 °C and 5% CO_2 in the air.

Imaging of Ca^{2+} oscillations

Oocytes loaded with 5 µM fluorescent Ca^{2+} indicator Oregon Green 488 BAPTA-1 AM (Molecular Probes, Thermo Fisher Scientific; in M2 medium, 30 min) were subjected to acidic Tyrode solution (pH 2.5) [35] to remove zonae pellucidae. Oocytes without zonae were transferred to a glass-bottom dish (MatTek Corporations) with 2 ml of M2 medium without BSA and allowed to stick to the glass bottom. Next, the dish was placed on a time-lapse imaging system (Zeiss Axiovert microscope with an AxioCam HRm camera) equipped with an environmental chamber sustaining a temperature of 37.5 °C. 1–2 µl of capacitated sperm suspension (approximate concentration of 2×10^7 spermatozoa/ml) were added to the oocytes. Time-lapse imaging was initiated ~17 h post hCG; single-plane images were taken every 10 s for ~7 h. Oocytes were illuminated with light passing through a 450–490 nm excitation filter, and the emitted light was collected with a 500–550 nm emission filter (exposure time 50 ms, 4 × 4 binning). Oocytes of each type (defined by the age and female strain) were imaged separately.

Changes in cytoplasmic Ca^{2+} concentration were assessed by measuring the mean intensity of Oregon Green BAPTA fluorescence in time. The Fiji software (https://imagej.net/Fiji) was used for the analysis. To avoid additional variability between the experiments caused by the different extent of dye loading (Supplementary Figure S1A), the initial (pre-fertilization) mean intensity of fluorescence was calculated for each oocyte and then used to normalize the measurements in this oocyte. The resulting values are ratios: measured fluorescence intensity (F)/initial fluorescence intensity (F_0). The rates of increase and decrease of Ca^{2+} concentration during the Ca^{2+} transients were calculated as tangents of the rising/decreasing slopes of the Ca^{2+} transients ("a" parameter in $y = ax + b$ linear function fitted into these slopes). The recordings were also analyzed for the timing of pronuclei formation (Oregon Green BAPTA dye does not accumulate in pronuclei, so they are visible as darker circular regions in the cell). To avoid the confounding effects of photobleaching and the dye compartmentalization that may appear during prolonged imaging, we analyzed only oocytes fertilized within the first 2 h of the recording, and we measured amplitudes only of the 1st and 3rd Ca^{2+} transients (Supplementary Figure S1B). Only monospermic oocytes were included in the final analysis and the number of fused sperm was assessed based on the number of fertilization cones and/or pronuclei formed. The numbers of analyzed oocytes and experimental repetitions are included in Supplementary Table S1.

Table 1. Ovulation yields in young and old females of different genetic backgrounds.

	Median (Q1; Q3)*Number of analyzed females*					
	F1		SWISS		C57BL/6	
Parameter	Young	Old	Young	Old	Young	Old
No. of ovulated oocytes per female	**36.5** (31.75; 45.25) *n = 18*	**1.5** [a] (0.4; 2.4) *n = 198*	**33.0** (21.0; 45.5) *n = 17*	**3.6** [a] (2.6; 5.3) *n = 49*	**23.0** (15.0; 33.0) *n = 13*	**1.8** [b] (1.6; 2.9) *n = 66*

[a] $P < 0.001$, [b] $P < 0.01$ vs. oocytes from young females of the respective background.

Ca^{2+} store measurement

Oocytes were loaded with 5 µM Oregon Green BAPTA-1 AM (in M2 medium, 30 min) and transferred to a glass-bottom dish with M2 medium devoid of Ca^{2+} and Mg^{2+} ions. After 2 minutes of time-lapse imaging thapsigargin (TG) or A23187 ionophore were added to the medium to the final concentration of 10 µM. Single-plane images were taken every 10 s for ~30 min (the settings were the same as described for imaging of Ca^{2+} oscillations). Oocytes of each type (defined by the age and female strain) were imaged separately.

Changes in the Oregon Green BAPTA fluorescence were analyzed as described for the imaging of Ca^{2+} oscillations. The amplitude of the Ca^{2+} transient (a difference between the maximum fluorescence intensity and the fluorescence intensity at the beginning of the Ca^{2+} increase) and the area under the curve (AUC) of the Ca^{2+} transient (calculated for the first 10 min following the onset of Ca^{2+} increase relative to baseline using the trapezoidal method; modified from [36]) were measured. All oocytes included in the analysis were viable at the end of the imaging period. The numbers of analyzed oocytes and experimental repetitions are included in Table 2.

Immunofluorescence staining

Oocytes were fixed for 30 min in room temperature (RT) in 4% formaldehyde solution prepared in PBS, permeabilized with (1) 0.2% Triton-X100 in PBS (25 min, RT) and blocked with 3% BSA in PBS for ITPR1 and calnexin stainings or (2) 0.5% Triton-X100 in PBS (25 min, RT) and blocked with 10% fetal bovine serum (FBS) solution prepared in PBS for ATP2A2 staining. Calnexin was labeled with a rabbit polyclonal antibody (Abcam, cat. no. ab22595; diluted 1:200 in 3% BSA) and ITPR1 with a rabbit polyclonal antibody (Abcam, cat. no. ab5908; diluted 1:100 in 3% BSA), both followed by an Alexa Fluor 633-conjugated goat anti-rabbit IgG (Invitrogen, Thermo Fisher Scientific, cat. no. A21071; diluted 1:200 in 3% BSA). ATP2A2 was labeled with a mouse monoclonal antibody (Abcam, cat. no. ab2861; diluted 1:100 in 10% FBS) followed by a TRITC-conjugated goat anti-mouse IgG (Jackson ImmunoResearch Laboratories Inc., cat. no. 115–025-068; diluted 1:200 in 10% FBS). Embryos were incubated in the primary antibodies overnight at 4 °C, washed in PBS and 3% BSA or 10% FBS, and then, incubated with the secondary antibody for 2 h in RT. Old and young oocytes were analyzed on an inverted confocal microscope (Zeiss and Olympus) using the same imaging settings. Mean fluorescence intensity was measured for the Z-stack projections prepared in the average intensity mode. The Fiji software was used for the analysis.

Western blotting

Expression of ITPR1 protein was examined in samples of 70–80 oocytes, depending on the experiment. Cell lysates were mixed with 4× NuPage LDS sample Buffer and 10× NuPage Sample Reducing Agent (Invitrogen, Thermo Fisher Scientific) and heated for 10 min in 70 °C. The samples were subjected to NuPage Novex 3–8% Tris-Acetate gels (Invitrogen, Thermo Fisher Scientific), and separated proteins were transferred onto PVDF membranes (Hyperbond-P, Amersham Biosciences). The blots were then stained with Ponceau S to confirm the equal sample load, blocked in 5% non-fat milk solution prepared in Tris-buffered saline with Tween20 (TTBS), and probed for 1 h with a rabbit polyclonal antibody (Rbt03) raised against a 15 amino acid peptide sequence of the C-terminal end of the ITPR1 [37] diluted 1:350 in 5% non-fat milk in TTBS. A goat anti-rabbit antibody (Bio-Rad) conjugated with horseradish peroxidase diluted 1:5000 was used as the secondary antibody in 1-h-long incubation. Detection was performed by the enhanced chemiluminescence technique using SuperSignal West Dura Extended Duration Substrate reagents (Pierce, Thermo Fisher Scientific) according to the manufacturer's instruction.

RT-qPCR

Oocytes were transferred in groups of 15–20 (depending on the experiment) into 20 µl of Lysis/Binding Buffer (Dynabeads mRNA DIRECT Micro Kit, Thermo Fisher Scientific) and stored in −80 °C until further analysis. mRNA was isolated from the samples using the Dynabeads mRNA DIRECT Micro Kit (Thermo Fisher Scientific) according to the manufacturer's protocol. In short, thawed samples were rotated with 10 µl of paramagnetic oligo-$(dT)_{25}$ bead suspension for 30 min at RT. mRNA was eluted from the beads by adding 10 µl of DEPC-treated water and heated for 10 min at 70 °C with 0.5 µg oligo$(dT)_{12–18}$. The reverse transcription was performed in a total volume of 20 µl using 200 U of Superscript II Reverse Transcriptase, 0.5 mM dNTPs, and 40 IU RNase inhibitor (Invitrogen, Thermo Fisher Scientific) at 42 °C for 50 min. Synthesized cDNA was diluted twice (to 40 µl) with nuclease-free water (Thermo Fisher Scientific) and subjected (3 µl per sample) to real-time PCR using TaqMan Gene Expression MasterMix and TaqMan Gene Expression Assays probes (*Itpr1/Ip3r1*: cat. no. Mm00439907_m1; *Atp2a2/Serca2*: Mm01275320_m1; *Erp44/Txndc4*: Mm00466483_m1; *Pdia3/Erp57*: Mm00433130_m; *Actb*: Mm01205647_g1; Applied Biosystems, Thermo Fisher Scientific) in StepOne Real-Time PCR System thermocycler (Applied Biosystems, Thermo Fisher Scientific; 50 °C/2 min; 60 °C/10 min; 50 cycles: 95 °C/15 s, 60 °C/1 min). The relative level of expression was calculated using the $2^{-\Delta Ct}$ method [38] with *Actb* expression used for normalization.

Statistical analysis

Normality of the data distribution was verified with the Shapiro–Wilk test. Data with a normal distribution were analyzed with the Student's *t*-test. When the distribution was not normal, we

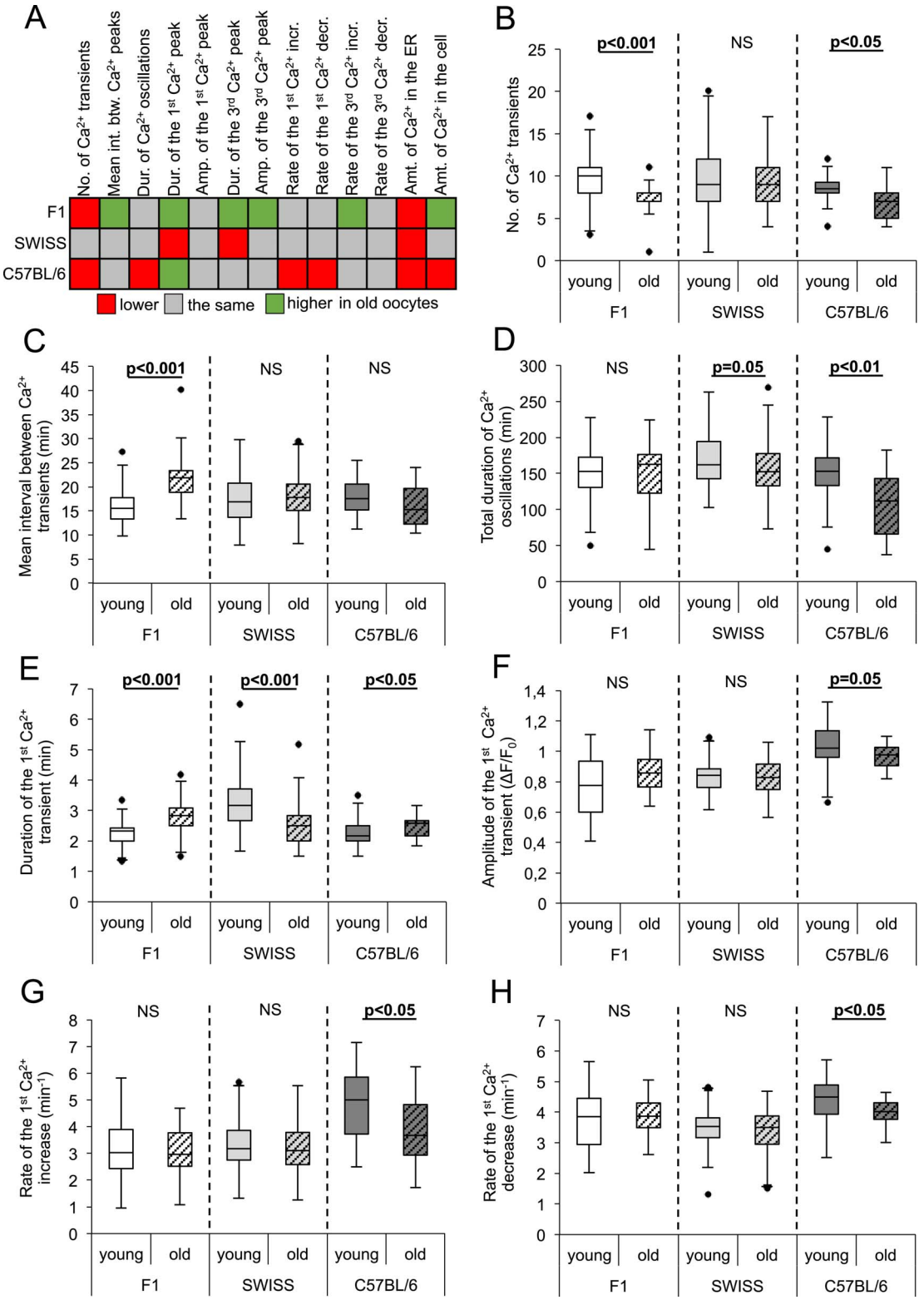

Figure 1. Effect of maternal aging on the pattern of fertilization-induced Ca^{2+} oscillations in oocytes from F1, SWISS, and C57BL/6 mice. (A) Summary of the alterations induced by maternal aging in Ca^{2+} oscillations in fertilized oocytes. Red marks values lower, gray—the same, and green—higher in old oocytes than in their young counterparts. The amounts of Ca^{2+} in the ER and the whole cell correspond to the AUCs for the TG- and A23187-induced Ca^{2+} increases, respectively. (B) The number of Ca^{2+} transients in young (n = 57 F1, 93 SWISS, 36 C57BL/6) and old (n = 30 F1, 74 SWISS, 17 C57BL/6) oocytes. (C) Mean interval between two consecutive Ca^{2+} transients calculated for the first 2 h of Ca^{2+} oscillations in young (n = 57 F1, 92 SWISS, 36 C57BL/6) and old (n = 29 F1, 74 SWISS, 17 C57BL/6) oocytes. (D) The total duration of Ca^{2+} oscillations in young (n = 57 F1, 92 SWISS, 36 C57BL/6) and old (n = 29 F1, 74 SWISS, 17 C57BL/6) oocytes. (E) Duration and (F) amplitude of the 1st Ca^{2+} transient in young (n = 55 F1, 92 SWISS, 36 C57BL/6) and old (n = 27 F1, 73 SWISS, 18 C57BL/6) oocytes. (G) Rate of Ca^{2+} increase during the 1st Ca^{2+} transient in young (n = 54 F1, 92 SWISS, 36 C57BL/6) and old (n = 27 F1, 74 SWISS, 18 C57BL/6) oocytes. (H) Rate

applied the Mann–Whitney U test. The differences between groups were considered statistically significant for $P < 0.05$. Spearman's rank correlation coefficient was used to show correlations between analyzed numerical variables.

Results

Maternal aging decreased ovulation yields in all examined genetic backgrounds

To examine the effects of maternal aging on oocytes' ability to generate correct Ca^{2+} response to fertilization, we needed to isolate MII oocytes. We noticed that reproductively aged females (13–16 months old, an equivalent of 36–45 years of age in humans [39]) of all three examined strains/crosses ovulated significantly fewer MII oocytes than their young counterparts (Table 1). This observation accords with the previously published data regarding the impact of maternal aging on mouse female fertility (e.g., [3, 19, 40–44]) and confirms that mice used in our experimental set-up indeed were in advanced reproductive age.

Maternal aging affects the pattern of Ca^{2+} oscillations in a strain-dependent manner

To investigate how advanced reproductive age affects the pattern of fertilization-induced Ca^{2+} oscillations, we labeled MII oocytes recovered from young and old F1, SWISS, and C57BL/6 females with Oregon Green 488 BAPTA-1 AM, a fluorescent Ca^{2+} indicator, fertilized them in vitro with F1 spermatozoa, and subjected them to time-lapse imaging. Next, we analyzed fluorescence intensity that reflected Ca^{2+} concentration in ooplasm and calculated several parameters describing the pattern of sperm-triggered Ca^{2+} oscillations, such as the number of Ca^{2+} transients, the mean interval between subsequent Ca^{2+} transients (the frequency of Ca^{2+} oscillations gradually decreases over time, so we calculated it only for the first 2 h after fertilization), the total duration of Ca^{2+} oscillations, the duration and amplitude of Ca^{2+} transients (we analyzed the 1st and the 3rd Ca^{2+} transients as examples), and the rate of increase/decrease of Ca^{2+} during the Ca^{2+} transients. As the number of fused sperm affects the pattern of Ca^{2+} oscillations [45], we included in our analysis only oocytes fertilized by a single sperm.

We showed that the pattern of Ca^{2+} oscillations was altered more severely in oocytes from old F1 and C57BL/6 mice than old SWISS mice. Maternal aging decreased the number and frequency of Ca^{2+} transients in F1 oocytes. However, the duration of Ca^{2+} transients (at least the 1st and the 3rd) was longer, and the amplitude and the rate of rise of the 3rd Ca^{2+} transient were higher in oocytes obtained from aged F1 females. In old C57BL/6 oocytes, Ca^{2+} oscillations lasted for shorter and consisted of fewer Ca^{2+} transients than in young oocytes. Moreover, the 1st Ca^{2+} peak in aged oocytes lasted on average for longer, and rates of its increase and decrease were slower than in young oocytes. SWISS oocytes were affected by the advanced maternal age to the lowest extent: in oocytes from old females, only the duration of the 1st and the 3rd Ca^{2+} transients was shorter than in oocytes from young females (Figure 1, Supplementary Table S1, Supplementary Figures S2 and S3).

It is important to note that our measurements of the amplitudes and, in consequence, also the rates of Ca^{2+} increase/decrease, are only estimates, as Oregon Green BAPTA is not a ratiometric dye, and its response to increasing Ca^{2+} concentration is not linear (its output flattens for higher Ca^{2+} concentrations) [46]. Therefore, we may have less ability to detect small differences in the amplitudes within the upper part of the dye working range. In summary, maternal aging alters the pattern of Ca^{2+} oscillations in fertilized oocytes in a different manner depending on the genetic background of the cells: F1 and C57BL/6 oocytes are more and SWISS oocytes less affected by the female advanced reproductive age.

Cellular Ca^{2+} store changes during maternal aging in a strain-dependent manner

It is possible that strain-dependent differences in the impact of maternal aging on the pattern of Ca^{2+} oscillations in fertilized oocytes are a consequence of different age-related alterations to the oocyte's Ca^{2+} store. Therefore, we examined whether the effect of maternal aging on the amount of Ca^{2+} stored in oocytes differed as well between the mouse strains. To this end, we labeled oocytes with Oregon Green 488 BAPTA-1 AM and treated them with thapsigargin (TG) or A23187 ionophore to assess Ca^{2+} amount stored in either ER cisterns or the whole cell, respectively. TG blocks ATP2A2 pump in the ER membrane and thus allows for a gradual leakage of Ca^{2+} from ER cisterns into the cytoplasm [47, 48]. On the other hand, A23187 ionophore is an ion-carrier that forms stable complexes with divalent cations and transports them across lipid bilayers such as cellular membranes [49]. Ca^{2+} increase induced by the reagents was recorded by time-lapse imaging, fluorescence intensity was analyzed, and amplitudes and areas under the curve (AUCs) for the Ca^{2+} transients were calculated.

We showed that maternal aging decreased the amount of Ca^{2+} accumulated in the ER, as assessed by the Ca^{2+} spike amplitude and AUC, in both F1 and C57BL/6 oocytes (Table 2, Figure 2A and C). It accords with our earlier observation that old F1 and C57BL/6 oocytes generated fewer Ca^{2+} transients in response to fertilization than their young counterparts and, additionally, that in old C57BL/6 oocytes Ca^{2+} oscillations lasted for shorter and in old F1 oocytes—were less frequent than in young oocytes (Figure 1B–D, Supplementary Table S1). The amplitude of TG-induced Ca^{2+} transient was increased, whereas the AUC was decreased in old SWISS oocytes comparing to their young counterparts (Table 2, Figure 2B). However, as the dynamics of Ca^{2+} response to TG was significantly different in young and old SWISS oocytes, the AUC of the Ca^{2+} transient is a better measure of the ER Ca^{2+} store than the Ca^{2+} transient amplitude. The slower Ca^{2+} response to TG observed for young SWISS oocytes suggests either lower responsiveness of ATP2A2 to the drug or decreased Ca^{2+} leak from the ER.

On the other hand, the amount of Ca^{2+} stored in the whole cell, as assessed by the amplitude and AUC of the Ca^{2+} response to A23187, was higher in oocytes from old F1 females and lower in oocytes from old C57BL/6 than in oocytes from their young counterparts (Table 2, Figure 2A and C). The amplitude of ionophore-induced Ca^{2+} transient was lower in old than in young SWISS oocytes, but the AUC remained the same in both types of oocytes. This suggests

Figure 1. (continued) of Ca^{2+} decrease during the 1st Ca^{2+} transient in young (n = 56 F1, 92 SWISS, 36 C57BL/6) and old (n = 30 F1, 74 SWISS, 16 C57BL/6) oocytes. (B–H) Graphs present medians and the 1st and the 3rd quartile values. The ends of the whiskers are set at 1.5∗IQR above the third quartile and 1.5∗IQR below the first quartile. Dots show the minimum and maximum values if they are outside the range (outliers).

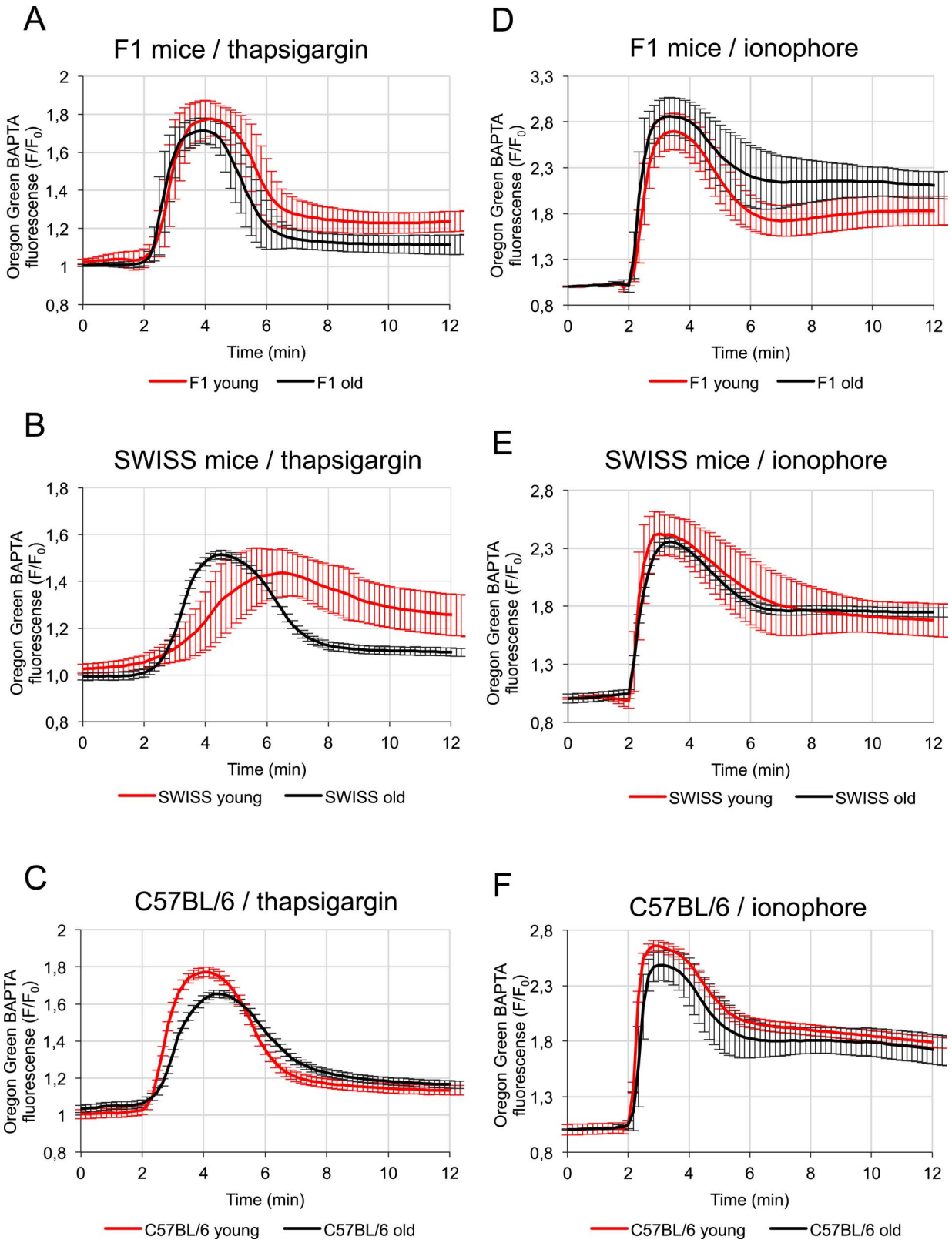

Figure 2. Effect of maternal aging on the amount of Ca^{2+} stored in oocytes from F1, SWISS and C57BL/6 mice. (A–C) Mean Ca^{2+} release triggered by thapsigargin (TG), calculated for young (in red; n = 52 F1, 48 SWISS, 44 C57BL/6) and old (in black; n = 26 F1, 30 SWISS, 25 C57BL/6) oocytes isolated from (A) F1, (B) SWISS, and (C) C57BL/6 mice. (D and E) Mean Ca^{2+} release triggered by A23187 ionophore, calculated for young (in red; n = 45 F1, 52 SWISS, 50 C57BL/6) and old (in black; n = 35 F1, 50 SWISS, 28 C57BL/6) oocytes isolated from (D) F1, (E) SWISS, and (F) C57BL/6 mice. Mean values ±SD are shown. Recordings were synchronized according to the time-point when the cytoplasmic Ca^{2+} concentration in oocytes started to rise.

Table 2. Amount of Ca^{2+} stored in oocytes obtained from young and old females of different genetic backgrounds.

	Median (Q1; Q3) *Number of analyzed embryos and number of experiments*					
	F1		SWISS		C57BL/6	
Parameter	Young	Old	Young	Old	Young	Old
Amplitude of Ca^{2+} transient triggered by TG ($\Delta F/F_0$)	**0.75** (0.68; 0.80) *n = 52, 2 exp*	**0.71** [c] (0.66; 0.74) *n = 26, 3 exp*	**0.43** (0.39; 0.47) *n = 48, 3 exp*	**0.53** [a] (0.47; 0.59) *n = 30, 3 exp*	**0.76** (0.71; 0.82) *n = 44, 2 exp*	**0.63** [a] (0.55; 0.70) *n = 25, 2 exp*
AUC of Ca^{2+} transient triggered by TG ($F/F_0 \times$ min)	**3.47** (3.20; 3.63) *n = 52, 2 exp*	**2.64** [a] (2.39; 2.93) *n = 26, 2 exp*	**2.60** (2.28; 3.15) *n = 48, 3 exp*	**2.36** [c] (1.65; 2.87) *n = 30, 3 exp*	**3.10** (2.77; 3.52) *n = 44, 2 exp*	**2.79** [b] (2.45; 3.06) *n = 25, 2 exp*
Amplitude of Ca^{2+} transient triggered by A23187 ($\Delta F/F_0$)	**1.64** (1.54; 1.77) *n = 45, 2 exp*	**1.89** [a] (1.68; 2.02) *n = 35, 2 exp*	**1.47** (1.35; 1.54) *n = 52, 2 exp*	**1.32** [a] (1.25; 1.39) *n = 50, 4 exp*	**1.61** (1.55; 1.71) *n = 50, 2 exp*	**1.46** [a] (1.36; 1.57) *n = 28, 3 exp*
AUC of Ca^{2+} transient triggered by A23187 ($F/F_0 \times$ min)	**9.31** (8.52; 10.16) *n = 45, 2 exp*	**12.24** [a] (11.34; 13.88) *n = 35, 2 exp*	**8.61** (8.00; 10.09) *n = 52, 2 exp*	**8.35** (7.55; 9.42) *n = 50, 4 exp*	**10.37** (9.61; 10.78) *n = 50, 2 exp*	**8.96** [b] (8.57; 10.12) *n = 17, 2 exp*

[a] $P < 0.001$, [b] $P < 0.01$, [c] $P < 0.05$ vs. oocytes obtained from young females of the respective genetic background.

that if there is any decrease in the amount of Ca^{2+} stored in the aged SWISS oocytes, it is relatively small (Table 2, Figure 2B). In summary, our data indicate that maternal aging decreases the ER Ca^{2+} store but, depending on the genetic background, may differently impact the amount of Ca^{2+} stored in other organelles (e.g., mitochondria).

Maternal aging affects the expression of Ca^{2+} homeostasis genes in a strain-depending manner but does not alter the distribution of ER cisterns

Alterations in the pattern of Ca^{2+} oscillations observed in oocytes obtained from aged females may be caused by changed expression of proteins involved in Ca^{2+} homeostasis. Pan and co-workers [3] and Grøndahl and co-workers [4] showed in their microarray analyses that maternal aging affects the expression of inositol 1,4,5-trisphosphate receptor 1 (*Itpr1*), ATPase sarcoplasmic/endoplasmic reticulum Ca2+ transporting 2 (*Atp2a2*), Endoplasmic reticulum resident protein 44 (*Erp44*), and Protein disulfide-isomerase A3 (*Pdia3*) genes in mice and humans, thus we decided to investigate the expression of these genes on mRNA and protein level in our experimental set-up. ITPR1 and ATP2A2 proteins regulate the flow of Ca^{2+} ions between ER cisterns and cytoplasm, whereas ERp44 and PDIA3 regulate ITPR1 and ATP2A2 activities, respectively (reviewed in [50]). Messenger RNA expression was assessed in ovulated MII oocytes, but because ovulation yield was very low in aged females, in the experiments detecting proteins we used GV oocytes isolated from ovaries and matured in vitro. To analyze mRNA expression, we isolate mRNAs using oligo $(dT)_{25}$-coated paramagnetic beads. The method is very effective for transcripts with poly(A) tails longer than 25 nts [51], but transcripts with shorter poly(A) tails might have been underrepresented in our analysis. The majority of mRNAs present in mammalian cells have on average longer poly(A) sequences (50–250 nts), but indeed, in oocytes, some maternal mRNAs stored for future translation may have short poly(A) tails; such tails usually mark mRNAs that are translationally dormant; therefore, even if present, they do not participate in the protein production at the given time-point (reviewed in [52, 53]).

The qPCR analysis indicated that in SWISS oocytes maternal aging did not change mRNA levels for any of the examined genes. In F1 oocytes, we noticed a decrease in mRNA expression of *Itpr1* and *Atp2a2*. However, it was not detectable on the protein level; on contrary, the ITPR and ATP2A2 expression seemed to be slightly higher in aged F1 oocytes (as assessed by immunofluorescence staining for ITPR1 and ATP2A2 and by Western blot for ITPR1; we did not manage to detect ATP2A2 signal in immunoblotting) (Figure 3A–F, Supplementary Figure S4). The cytoplasmic distribution of ITPR1 and ATP2A2 observed by us in the immunostainings accords with the data published previously [54, 55] and mirrors the distribution of calnexin, an ER marker (Figure 3E and G). Interestingly, we did not observe an upshift in the position of the ITPR1 band in samples from old vs. samples from young oocytes, which indicates that maternal aging did not lead to abundant phosphorylation of the ITPR1 protein [56, 57] (Figure 3F). In oocytes obtained from C57BL/6 females, maternal aging led to a decline in the expression of *Erp44* mRNA. Unfortunately, we were able to detect ERp44 protein neither by immunostaining nor by Western blot, so we cannot verify whether the aging impacts the protein amount (Figure 3A–F).

The dynamics of Ca^{2+} oscillations may also depend on the distribution of the ER cisterns [56–58]. Therefore, we examined

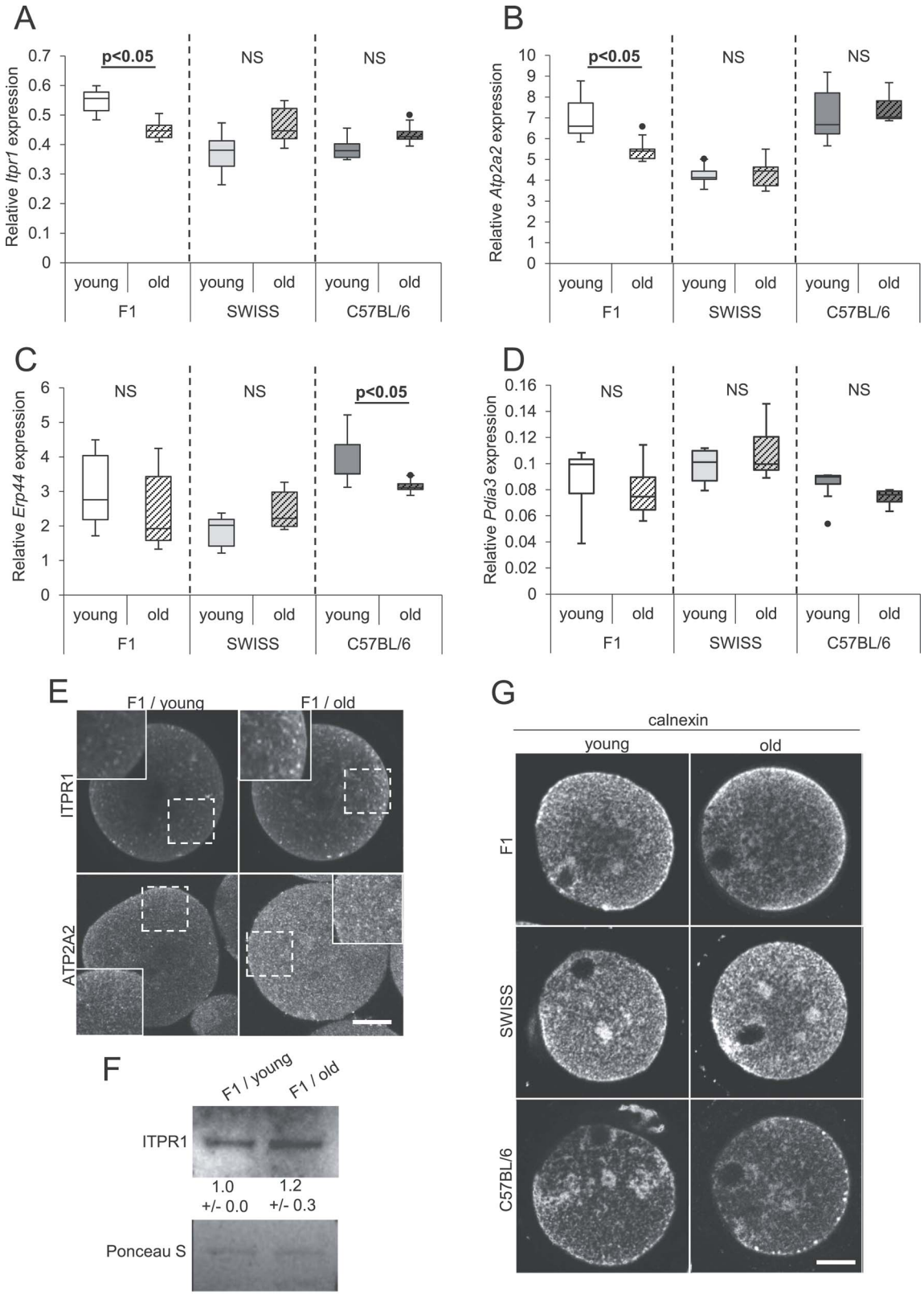

Figure 3. Distribution of ER cisterns and expression of genes involved in Ca^{2+} homeostasis in oocytes from young and old F1, SWISS, and C57BL/6 mice. (A–D) Relative expression of mRNA for (A) *Itpr1*, (B) *Atp2a2*, (C) *Erp44*, and (D) *Pdia3* genes in young and old oocytes. PCR analysis was repeated six times. (E) Representative images of immunofluorescence stainings for ITPR1 and ATP2A2 in F1 young (n = 49 and 29, respectively) and old (n = 13 and 28, respectively) oocytes. Regions marked with dashed line are magnified in the inserts. Scale bar 20 μm. (F) Western blot analysis for ITPR1 in F1 young and old oocytes. Numbers below the blots present mean results (±SD) of the densitometric analysis from three experiments. Ponceau S staining was used to confirm an equal sample loading. (F) Representative images of immunofluorescence stainings for calnexin, the ER marker, in young (n = 29 F1, 18 SWISS, 12 C57BL/6) and old (n = 34 F1, 20 SWISS, 8 C57BL/6) oocytes.

whether maternal aging changes the distribution of the ER network in MII oocytes. As before, we used MII oocytes that matured in vitro, and we labeled them for calnexin, an ER marker. Our analysis indicated that ER cisterns were distributed as previously shown [56, 57, 59] and that maternal aging did not affect their localization, regardless of the female's genetic background (Figure 3G).

Taken together, even though we detected some age-related differences in mRNA expression of genes involved in Ca^{2+} homeostasis, those differences did not necessarily translate directly to protein levels. Moreover, maternal aging did not affect the distribution of ER cisterns. Consequently, neither of those parameters can fully explain the age-dependent change in the pattern of Ca^{2+} oscillations.

Maternal aging alters the timing of pronuclei formation in a strain-dependent manner

As the pattern of Ca^{2+} oscillations regulates early embryonic cell cycle events [9, 10], we wished to examine whether age-related modifications in Ca^{2+} oscillations coincide with altered timing of pronuclei formation in zygotes. To this end, we measured the time between the initiation of the first Ca^{2+} transient and the first appearance of pronuclei in zygotes obtained from young and aged F1, SWISS, and C57BL/6 females. We observed that pronuclei formed later in zygotes from old F1 and SWISS females than in embryos from their young counterparts, whereas in CB57BL/6 zygotes we noticed the opposite trend (Figure 4A). It has been shown that the events accompanying oocyte activation rely on the total duration of the period when the cytoplasmic Ca^{2+} concentration is increased [9, 10]. Therefore, we examined whether the timing of pronuclei formation correlates with the number of Ca^{2+} transients and the mean period between subsequent Ca^{2+} transients (translating to the frequency of Ca^{2+} oscillations), as these parameters reflect the total time when the cytoplasmic Ca^{2+} concentration is elevated. Old and young oocytes were analyzed together and a significant positive correlation was observed only between the timing of pronuclei formation and the mean period between subsequent Ca^{2+} transients for C57BL/6 and SWISS strains (Figure 4B). Therefore, our results suggest that the frequency of sperm-induced Ca^{2+} oscillations may affect the timing of pronuclei formation at least in some mouse strains. However, as the frequency of Ca^{2+} peaks did not actually differ between young and old oocytes from C57BL/6 and SWISS mice, there must be another factor(s) that explains the different rates of interphase onset in embryos obtained from young and old females.

Discussion

In our study, we investigated the effect of female age on Ca^{2+} homeostasis in oocytes of different genetic backgrounds. It is important to note that in mice aging is usually accompanied by various physiological changes occurring simultaneously in the organism, e.g., metabolic alterations that lead to overweight (observed in our aged females as well, data not shown). Indeed, Selesniemi and co-workers showed that some aging-related oocyte defects can be rescued by caloric restriction or deletion of PGC-1α, a transcriptional regulator highly responsive to nutritional cues [43]. In our experimental set-up, it was difficult to separate the effects of pure age from the effects of accompanying conditions, so in the present paper, we treated them collectively and referred to as maternal aging.

We showed that maternal aging impairs the sperm-induced Ca^{2+} oscillations in oocytes, but the direction and extent of these alterations depend on the genetic origin of the females (Figure 1A). In general, the Ca^{2+} oscillatory pattern in oocytes obtained from aged C57BL/6 and F1 mouse females was more disturbed than in oocytes from old SWISS females. Aged C57BL/6 females were used before the experiments as breeders (whereas aged females of other genetic backgrounds were not), which might be a confounding factor. However, it has been suggested that alterations induced by maternal aging in mammalian oocytes are predominantly caused by oxidative stress, and the process of ovulation stimulates the production of reactive oxygen species (ROS) in ovaries [60–62]. Therefore, aged breeder females that experienced a limited number of ovulatory cycles could have oocytes of higher quality than aged females that ovulated more frequently. Still, oocytes obtained from old C57BL/6 females seemed to be rather severely affected by maternal aging comparing to oocytes from old females of other genetic backgrounds. Our observations correspond well with other reports on phenotypical variability between oocytes/embryos of different mouse strains. It has been indicated that the genetic background of mice affects oocytes and embryos' ability to develop in vitro and in vivo [20–30]. Moreover, embryos originating from oocytes of different mouse strains display distinct epigenetic modifications not only in maternal but also paternal genome [63–65] and may differ in the protein expression levels [66]. Interestingly, it has been reported recently that oocytes from young females of various genetic origins accumulate different amounts of Ca^{2+} and display different patterns of fertilization-induced Ca^{2+} oscillations [36], which accords well with the results presented here.

We also showed that the altered pattern of Ca^{2+} oscillations in fertilized oocytes of older females is accompanied by the altered timing of the initiation of the 1st embryonic interphase. Our data suggest that in some mouse strains there is a relationship between the frequency of Ca^{2+} oscillations and the timing of pronuclei formation, although it is not necessarily responsible for the differences in the timing of interphase onset between young and old oocytes. This observation accords with the previously reported results indicating that the pattern of Ca^{2+} oscillations regulates completion of meiosis and initiation of embryonic divisions and that a certain threshold number of Ca^{2+} transients is necessary to induce the formation of pronuclei [9, 10]. Moreover, the frequency of Ca^{2+} oscillations has been reported to correlate with various morphokinetic parameters at post-zygotic stages [67]. Interestingly, in contrast to zygotes obtained from old F1 and SWISS oocytes, zygotes from old C57BL/6 oocytes enter the 1st mitotic interphase faster than their counterparts from young oocytes. C57BL/6 oocytes have been reported as particularly prone to spontaneous parthenogenetic activation [68]. Although each C57BL/6 substrain may display different phenotype, it is possible that with age oocytes from our C57BL/6 substrain (C57BL/6Tar) become more susceptible to parthenogenetic activation, which can be reflected by the accelerated pronuclei formation. It would be interesting to investigate whether the altered pattern of Ca^{2+} oscillations observed in maternally aged oocytes correlates with other changes in their developmental capacity. Indeed, it has been shown that altered number and frequency of Ca^{2+} transients may translate to modified gene expression at the blastocyst stage and decreased capacity of the embryos to implant and develop to term [11].

Our results raised the question, why Ca^{2+} oscillations in oocytes from aged females of different mouse strains were differently affected. It seems that it can be partially explained by the impact of maternal aging on oocyte's ability to accumulate Ca^{2+} in the ER cisterns. Aged oocytes of all examined genetic backgrounds stored less Ca^{2+} in the ER than the young ones. Accordingly, F1 and C57BL/6 old oocytes generated on average fewer Ca^{2+} transients in

A

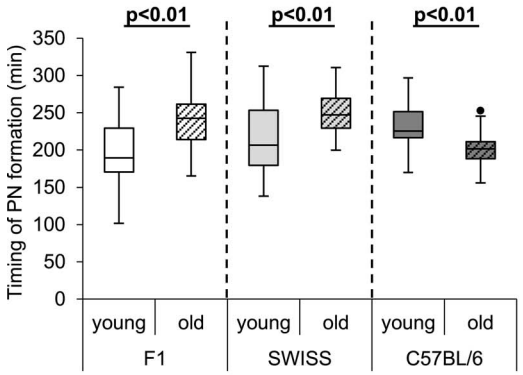

B

Time of PN formation vs.

Mean interval between Ca^{2+} transients (the first 2 hrs)

	No. of embryos	r	p-value
F1	39 (26 young and 13 old)	0.15	0.37
SWISS	61 (39 young and 22 old)	**0.33**	**0.01**
C57BL/6	38 (27 young and 11 old)	**0.40**	**0.01**

Numer of Ca^{2+} transients

	No. of embryos	r	p-value
F1	39 (26 young and 13 old)	0.08	0.63
SWISS	61 (39 young and 22 old)	0.13	0.31
C57BL/6	38 (27 young and 11 old)	0.05	0.78

Figure 4. Timing of the pronuclei formation in fertilized oocytes from young and old F1, SWISS, and C57BL/6 mice. (A) Timing of pronuclei formation in young (n = 26 F1, 41 SWISS, 28 C57BL/6) and old (n = 13 F1, 22 SWISS, 12 C57BL/6) fertilized oocytes. The graph presents medians and the 1st and the 3rd quartile values. The ends of the whiskers are set at 1.5∗IQR above the third quartile and 1.5∗IQR below the first quartile. Dots show the minimum and maximum values if they are outside the range (outliers). (B) Correlation between the mean interval between Ca^{2+} transients (within the first 2 h of Ca^{2+} oscillations) or the number of Ca^{2+} transients and the timing of pronuclei formation for fertilized oocytes obtained from F1, SWISS, and C57BL/6 females.

response to fertilization. Additionally, in old F1 oocytes, Ca^{2+} transients were less frequent, in old C57BL/6 oocytes Ca^{2+} oscillations ceased faster, and in old SWISS oocytes, the duration of the 1st Ca^{2+} transient was shorter than in their young counterparts. However, cytoplasmic Ca^{2+} increase in response to TG treatment most likely does not fully reflect the ER Ca^{2+} stores and the egg contains a TG-insensitive or TG-resistant pool that may be mobilized by sperm at fertilization [48]. Moreover, it seems plausible that other factors are also responsible for the differences in the Ca^{2+} oscillatory patterns in oocytes from young and old females. Haverfield and co-workers [19] showed that oocytes from aged CD1 females had an impaired ability to transport Ca^{2+} ions from the environment into the cytoplasm. Ca^{2+} influx is necessary to sustain the long-lasting Ca^{2+} oscillations in fertilized oocytes [48, 69, 70], so if this mechanism is differently affected in aged oocytes of various genetic backgrounds, this could explain at least some of the differences in the extent and direction of the alterations in their Ca^{2+} oscillatory patterns.

Amplitudes and durations of Ca^{2+} transients, as well as their rates of increase and decrease, may depend also on the amount and functionality of ITPR1 and ATP2A2 proteins. Similarly, the different dynamics of response to TG observed for SWISS young oocytes, as compared to the old ones, suggests decreased responsiveness of ATP2A2 to the drug or/and a slower rate of the TG-induced Ca^{2+} leak caused by an altered functionality of the Ca^{2+} channels involved in this process. In old C57BL/6 and SWISS oocytes, the expression of *Itpr1* and *Atp2a2* (on mRNA level) was comparable to the expression in young oocytes. In F1 oocytes we observed an age-related decline in the amounts of *Itpr1* and *Atp2a2* mRNAs (at least those sufficiently polyadenylated), but the amount of ITPR1 and ATP2A2 proteins seemed to be higher in old F1 oocytes. This could suggest that in aged F1 females, translation of ITPR1 and ATP2A2 occurs more intensely during oocyte maturation, or the proteins are more stable. Noteworthy, there is a possibility that maternal aging leads to posttranslational modifications that alter the activities of these proteins. ITPR1 functionality, particularly its sensitivity to IP_3, depends on the phosphorylation status of the receptor [71–73]. MAPK and MPF are the key kinases phosphorylating ITPR1 and stimulating its action [71, 73, 74]. It has been reported that maternal aging affects their activity, and it seems that the effect may be strain-dependent. Manosalva and Gonzalez [75] showed that MPF activity is decreased in oocytes obtained from old CD1 females. On the other hand, Tarin and co-workers [76] reported an elevation in MPF and MAPK activities in oocytes from aged F1(C57BL/6 × CBA) females, but our Western blot analysis did not reveal an upshift in the position of the ITPR1 bands obtained for the old F1 oocytes, typical for abundantly phosphorylated protein [59, 71].

Activities of both ITPR1 and ATP2A2 depend also on the redox status of the cell (reviewed in [77]). It has been reported repeatedly that maternal aging leads to elevation of the ROS level in oocytes (e.g., [78–81]). Therefore, if susceptibility of oocytes obtained from different mouse strains to aging-related oxidative stress varies, the redox-associated modifications of ITPR1 and ATP2A2 and, in consequence, the pattern of Ca^{2+} oscillations may also differ. In C57BL/6 oocytes maternal aging decreased also *Erp44* mRNA level, which could translate to an altered amount of ERp44 protein. ERp44 belongs to the thioredoxin protein family and interacts with one of the lumenal loops of ITPR1 in Ca^{2+}- and redox state-dependent way and inhibits the Ca^{2+} release through the receptor when the concentration of Ca^{2+} ions inside the ER cisterns decreases [82]. It, therefore, regulates the duration of the Ca^{2+} transients. Interestingly, in aged C57BL/6 oocytes, the first Ca^{2+} transient was longer than in their young counterparts, which could be expected if indeed the amount of ERp44 protein was decreased. Finally, as there is a tight and bi-directional relationship between mitochondrial activity and generation of Ca^{2+} oscillations (reviewed in [83, 84]), it is also possible that different susceptibility of Ca^{2+} oscillations to maternal aging reflects the impact of the female's age on the functionality of mitochondria. It has been shown in oocytes of various mouse strains that maternal aging leads to the formation of mitochondria aggregates and a decrease in the mtDNA copy number and mitochondrial activity [43, 81, 85–89]. Moreover, transcriptomic analyses revealed that the expression of genes involved in oxidative phosphorylation and energy metabolism is often misregulated in oocytes from aged mouse females [2, 3, 6].

In summary, our results indicate that the impact of maternal aging on oocyte quality—in our case assessed as its ability to generate a certain pattern of Ca^{2+} oscillations in response to fertilization—differs depending on the genetic background of the mouse female. They prove that interpretation of oocyte/embryo physiological response to aging, and most likely other environmental conditions, requires caution and a multidirectional approach to reveal the biological truth.

Supplementary data

Supplementary data is available at *BIOLRE* online.

Acknowledgments

We would like to thank Dariusz Maluchnik and Aleksander Chlebowski for their assistance in the oocyte imaging.

Author contributions

AA and KC designed the experiments. KC conducted the majority of experiments and performed the initial data analysis. AW and TI performed experiments concerning ITPR1 expression in F1 oocytes. KS supervised and consulted the RT-qPCR experiments. AA secured the funding, performed the final data analysis, and wrote the manuscript.

References

1. Qiao J, Wang ZB, Feng HL, Miao YL, Wang Q, Yu Y, Wei YC, Yan J, Wang WH, Shen W, Sun SC, Schatten H et al. The root of reduced fertility in aged women and possible therapeutic options: current status and future prospects. *Mol Aspects Med* 2014; **38**:54–85.
2. Hamatani T, Falco G, Carter MG, Akutsu H, Stagg CA, Sharov AA, Dudekula DB, VanBuren V, Ko MS. Age-associated alteration of gene expression patterns in mouse oocytes. *Hum Mol Genet* 2004; **13**:2263–2278.
3. Pan H, Ma P, Zhu W, Schultz RM. Age-associated increase in aneuploidy and changes in gene expression in mouse eggs. *Dev Biol* 2008; **316**:397–407.
4. Grøndahl ML, Yding Andersen C, Bogstad J, Nielsen FC, Meinertz H, Borup R. Gene expression profiles of single human mature oocytes in relation to age. *Hum Reprod* 2010; **25**:957–968.
5. Schwarzer C, Siatkowski M, Pfeiffer MJ, Baeumer N, Drexler HC, Wang B, Fuellen G, Boiani M. Maternal age effect on mouse oocytes: new biological insight from proteomic analysis. *Reproduction* 2014; **148**:55–72.
6. Zhang T, Xi Q, Wang D, Li J, Wang M, Li D, Zhu L, Jin L. Mitochondrial dysfunction and endoplasmic reticulum stress involved in oocyte aging: an analysis using single-cell RNA-sequencing of mouse oocytes. *J Ovarian Res* 2019; **12**:53.
7. Bentov Y, Yavorska T, Esfandiari N, Jurisicova A, Casper RF. The contribution of mitochondrial function to reproductive aging. *J Assist Reprod Genet* 2011; **28**:773–783.
8. Cimadomo D, Fabozzi G, Vaiarelli A, Ubaldi N, Ubaldi FM, Rienzi L. Impact of maternal age on oocyte and embryo competence. *Front Endocrinol (Lausanne)* 2018; **9**:327.
9. Ducibella T, Huneau D, Angelichio E, Xu Z, Schultz RM, Kopf GS, Fissore R, Madoux S, Ozil JP. Egg-to-embryo transition is driven by differential responses to Ca^{2+} oscillation number. *Dev Biol* 2002; **250**:280–291.
10. Ozil JP, Markoulaki S, Toth S, Matson S, Banrezes B, Knott JG, Schultz RM, Huneau D, Ducibella T. Egg activation events are regulated by the duration of a sustained $[Ca^{2+}]$cyt signal in the mouse. *Dev Biol* 2005; **282**:39–54.
11. Ozil JP, Banrezes B, Toth S, Pan H, Schultz RM. Ca^{2+} oscillatory pattern in fertilized mouse eggs affects gene expression and development to term. *Dev Biol* 2006; **300**:534–544.
12. Ducibella T, Schultz RM, Ozil JP. Role of calcium signals in early development. *Semin Cell Dev Biol* 2006; **17**:324–332.
13. Saunders CM, Larman MG, Parrington J, Cox LJ, Royse J, Blayney LM, Swann K, Lai FA. PLC zeta: a sperm-specific trigger of Ca(2+) oscillations in eggs and embryo development. *Development* 2002; **129**:3533–3544.
14. Fissore RA, Longo FJ, Anderson E, Parys JB, Ducibella T. Differential distribution of inositol trisphosphate receptor isoforms in mouse oocytes. *Biol Reprod* 1999; **60**:49–57.
15. Berridge MJ, Bootman MD, Roderick HL. Calcium signalling: dynamics, homeostasis and remodelling. *Nat Rev Mol Cell Biol* 2003; **4**:517–529.
16. Larman MG, Saunders CM, Carroll J, Lai FA, Swann K. Cell cycle-dependent Ca^{2+} oscillations in mouse embryos are regulated by nuclear targeting of PLCzeta. *J Cell Sci* 2004; **117**:2513–2521.
17. Yoda A, Oda S, Shikano T, Kouchi Z, Awaji T, Shirakawa H, Kinoshita K, Miyazaki S. Ca^{2+} oscillation-inducing phospholipase C zeta expressed in mouse eggs is accumulated to the pronucleus during egg activation. *Dev Biol* 2004; **268**:245–257.
18. Cooney MA, Malcuit C, Cheon B, Holland MK, Fissore RA, D'Cruz NT. Species-specific differences in the activity and nuclear localization of murine and bovine phospholipase C zeta 1. *Biol Reprod* 2010; **83**:92–101.
19. Haverfield J, Nakagawa S, Love D, Tsichlaki E, Nomikos M, Lai FA, Swann K, FitzHarris G. Ca^{2+} dynamics in oocytes from naturally-aged mice. *Sci Rep* 2016; **6**:19357.
20. Polański Z. In-vivo and in-vitro maturation rate of oocytes from two strains of mice. *J Reprod Fertil* 1986; **78**:103–109.
21. Fissore RA, Jackson KV, Kiessling AA. Mouse zygote development in culture medium without protein in the presence of ethylenediaminetetraacetic acid. *Biol Reprod* 1989; **41**:835–841.
22. Chatot CL, Lewis JL, Torres I, Ziomek CA. Development of 1-cell embryos from different strains of mice in CZB medium. *Biol Reprod* 1990; **42**:432–440.
23. Spindle A. In vitro development of one-cell embryos from outbred mice: influence of culture medium composition. *In Vitro Cell Dev Biol* 1990; **26**:151–156.
24. Du ZF, Wales RG. Some effects of genotype and composition of the culture medium on the development of mouse zygotes in vitro. *Reprod Fertil Dev* 1993; **5**:405–415.
25. Scott L, Whittingham DG. Influence of genetic background and media components on the development of mouse embryos in vitro. *Mol Reprod Dev* 1996; **43**:336–346.
26. Polański Z. Genetic background of the differences in timing of meiotic maturation in mouse oocytes: a study using recombinant inbred strains. *J Reprod Fertil* 1997; **109**:109–114.
27. Gao S, Czirr E, Chung YG, Han Z, Latham KE. Genetic variation in oocyte phenotype revealed through parthenogenesis and cloning: correlation with differences in pronuclear epigenetic modification. *Biol Reprod* 2004; **70**:1162–1170.
28. Ibánez E, Albertini DF, Overström EW. Effect of genetic background and activating stimulus on the timing of meiotic cell cycle progression in parthenogenetically activated mouse oocytes. *Reproduction* 2005; **129**:27–38.
29. Ozawa Y, Watanabe K, Toda T, Shibuya S, Okumura N, Okamoto N, Sato Y, Kawashima I, Kawamura K, Shimizu T. Heterosis extends the reproductive ability in aged female mice. *Biol Reprod* 2019; **100**:1082–1089.
30. Yamauchi Y, Ajduk A, Ward MA. Oocytes from female mice on MF1 genetic background are not suitable for assisted reproduction. *Biol Reprod* 2020; **102**:521–523.
31. Giuliani C, Pirazzini C, Delledonne M, Xumerle L, Descombes P, Marquis J, Mengozzi G, Monti D, Bellizzi D, Passarino G, Luiselli D, Franceschi C et al. Centenarians as extreme phenotypes: an ecological perspective to get insight into the relationship between the genetics of longevity and age-associated diseases. *Mech Aging Dev* 2017; **165**:195–201.
32. Revelas M, Thalamuthu A, Oldmeadow C, Evans TJ, Armstrong NJ, Kwok JB, Brodaty H, Schofield PR, Scott RJ, Sachdev PS, Attia JR, Mather

KA. Review and meta-analysis of genetic polymorphisms associated with exceptional human longevity. *Mech Aging Dev* 2018; **175**:24–34.
33. Fulton BP, Whittingham DG. Activation of mammalian oocytes by intracellular injection of calcium. *Nature* 1978; **273**:149–151.
34. Fraser L. Ca^{2+} is required for mouse sperm capacitation and fertilization in vitro. *J Androl* 1982; **3**:412–419.
35. Nicolson GL, Yanagimachi R, Yanagimachi H. Ultrastructural localization of lectin-binding sites on the zonae pellucidae and plasma membranes of mammalian eggs. *J Cell Biol* 1975; **66**:263–274.
36. McDonough CE, Bernhardt ML, Williams CJ. Mouse strain-dependent egg factors regulate calcium signals at fertilization. *Mol Reprod Dev* 2020; **87**:284–292.
37. Parys JB, de Smedt H, Missiaen L, Bootman MD, Sienaert I, Casteels R. Rat basophilic leukemia cells as model system for inositol 1,4,5-trisphosphate receptor IV, a receptor of the type II family: functional comparison and immunological detection. *Cell Calcium* 1995; **17**:239–249.
38. Livak KJ, Schmittgen TD. Analysis of relative gene expression data using real-time quantitative PCR and the 2(−Delta DeltaC(T)) method. *Methods* 2001; **25**:402–408.
39. Camlin NJ, McLaughlin EA, Holt JE. The use of C57Bl/6 × CBA F1 hybrid cross as a model for human age-related oocyte aneuploidy. *Mol Reprod Dev* 2017; **84**:6–7.
40. Zuccotti M, Boiani M, Garagna S, Redi CA. Analysis of aneuploidy rate in Antral and ovulated mouse oocytes during female aging. *Mol Reprod Dev* 1998; **50**:305–312.
41. Tarin JJ, Perez-Albala S, Cano A. Cellular and morphological traits of oocytes retrieved from aging mice after exogenous ovarian stimulation. *Biol Reprod* 2001; **65**:141–150.
42. Yan J, Suzuki J, Yu X, Kan FWK, Qiao J, Chian RC. Cryo-survival, fertilization and early embryonic development of vitrified oocytes derived from mice of different reproductive age. *J Assist Reprod Genet* 2010; **27**:605–611.
43. Selesniemi K, Lee HJ, Muhlhauser A, Tilly JL. Prevention of maternal aging-associated oocyte aneuploidy and meiotic spindle defects in mice by dietary and genetic strategies. *Proc Natl Acad Sci USA* 2011; **108**:12319–12324.
44. Fu X, Cheng J, Hou Y, Zhu S. The association between the oocyte pool and aneuploidy: a comparative study of the reproductive potential of young and aged mice. *J Assist Reprod Genet* 2014; **31**:323–331.
45. Faure JE, Myles DG, Primakoff P. The frequency of calcium oscillations in mouse eggs at fertilization is modulated by the number of fused sperm. *Dev Biol* 1999; **213**:370–377.
46. Johnson I, Spence MTZ (eds.). *The Molecular Probes Handbook*, 11th ed. Life Technologies Corporation; 2010: 829–882.
47. Wictome M, Henderson I, Lee AG, East JM. Mechanism of inhibition of the calcium pump of sarcoplasmic reticulum by thapsigargin. *Biochem J* 1992; **283**:525–529.
48. Kline D, Kline JT. Thapsigargin activates a calcium influx pathway in the unfertilized mouse egg and suppresses repetitive calcium transients in the fertilized egg. *J Biol Chem* 1992; **267**:17624–17639.
49. Erdahl WL, Chapman CJ, Taylor RW, Pfeiffer DR. Ca^{2+} transport properties of ionophores A23187, ionomycin, and 4-BrA23187 in a well defined model system. *Biophys J* 1994; **66**:1678–1693.
50. Ajduk A, Małagocki A, Maleszewski M. Cytoplasmic maturation of mammalian oocytes: development of a mechanism responsible for sperm-induced Ca^{2+} oscillations. *Reprod Biol* 2008; **8**:3–22.
51. Meijer HA, Bushell M, Hill K, Gant TW, Willis AE, Jones P, de Moor CH. A novel method for poly(A) fractionation reveals a large population of mRNAs with a short poly(A) tail in mammalian cells. *Nucleic Acids Res* 2007; **35**:e132.
52. Jalkanen AL, Coleman SJ, Wilusz J. Determinants and implications of mRNA poly(A) tail size - does this protein make my tail look big? *Semin Cell Dev Biol* 2014; **34**:24–32.
53. Tian B, Manley JL. Alternative polyadenylation of mRNA precursors. *Nat Rev Mol Cell Biol* 2017; **18**:18–30.
54. Wakai T, Zhang N, Vangheluwe P, Fissore RA. Regulation of endoplasmic reticulum Ca^{2+} oscillations in mammalian eggs. *J Cell Sci* 2013; **126**:5714–5724.
55. Yoon SY. Role of type 1 inositol 1,4,5-triphosphate receptors in mammalian oocytes. *Dev Reprod* 2019; **23**:1–9.
56. Fitzharris G, Marangos P, Carroll J. Cell cycle-dependent regulation of structure of endoplasmic reticulum and inositol 1,4,5-trisphosphate-induced Ca^{2+} release in mouse oocytes and embryos. *Mol Biol Cell* 2003; **14**:288–301.
57. FitzHarris G, Marangos P, Carroll J. Changes in endoplasmic reticulum structure during mouse oocyte maturation are controlled by the cytoskeleton and cytoplasmic dynein. *Dev Biol* 2007; **305**:133–144.
58. Kim B, Zhang X, Kan R, Cohen R, Mukai C, Travis AJ, Coonrod SA. The role of MATER in endoplasmic reticulum distribution and calcium homeostasis in mouse oocytes. *Dev Biol* 2014; **386**:331–339.
59. Wakai T, Vanderheyden V, Yoon SY, Cheon B, Zhang N, Parys JB, Fissore RA. Regulation of inositol 1,4,5-trisphosphate receptor function during mouse oocyte maturation. *J Cell Physiol* 2012; **227**:705–717.
60. Tatone C, Amicarelli F. The aging ovary—the poor granulosa cells. *Fertil Steril* 2013; **99**:12–17.
61. Miyamoto K, Sato EF, Kasahara E, Jikumaru M, Hiramoto K, Tabata H, Katsuragi M, Odo S, Utsumi K, Inoue M. Effect of oxidative stress during repeated ovulation on the structure and functions of the ovary, oocytes, and their mitochondria. *Free Radic Biol Med* 2010; **49**:674–681.
62. Shkolnik K, Tadmor A, Ben-Dor S, Nevo N, Galiani D, Dekel N. Reactive oxygen species are indispensable in ovulation. *Proc Natl Acad Sci USA* 2011; **108**:1462–1467.
63. Latham KE, Solter D. Effect of egg composition on the developmental capacity of androgenetic mouse embryos. *Development* 1991; **113**:561–568.
64. Latham KE. Strain-specific differences in mouse oocytes and their contributions to epigenetic inheritance. *Development* 1994; **120**:3419–3426.
65. Latham KE, Sapienza C. Localization of genes encoding egg modifiers of paternal genome function to mouse chromosomes one and two. *Development* 1998; **125**:929–935.
66. Pfeiffer MJ, Taher L, Drexler H, Suzuki Y, Makałowski W, Schwarzer C, Wang B, Fuellen G, Boiani M. Differences in embryo quality are associated with differences in oocyte composition: a proteomic study in inbred mice. *Proteomics* 2015; **15**:675–687.
67. Milewski R, Szpila M, Ajduk A. Dynamics of cytoplasm and cleavage divisions correlates with preimplantation embryo development. *Reproduction* 2018; **155**:1–14.
68. Cheng Y, Zhong Z, Latham KE. Strain specific spontaneous activation during mouse oocyte maturation. *Fertil Steril* 2012; **98**:200–206.
69. Igusa Y, Miyazaki S. Effects of altered extracellular and intracellular calcium concentration on hyperpolarizing responses of the hamster egg. *J Physiol* 1983; **340**:611–632.
70. Bernhardt ML, Stein P, Carvacho I, Krapp C, Ardestani G, Mehregan A, Umbach DM, Bartolomei MS, Fissore RA, Williams CJ. TRPM7 and CaV3.2 channels mediate Ca^{2+} influx required for egg activation at fertilization. *Proc Natl Acad Sci USA* 2018; **115**:E10370–E10378.
71. Lee B, Vermassen E, Yoon SY, Vanderheyden V, Ito J, Alfandari D, De Smedt H, Parys JB, Fissore RA. Phosphorylation of IP3R1 and the regulation of [Ca2+]i responses at fertilization: a role for the MAP kinase pathway. *Development* 2006; **133**:4355–4365.
72. Vanderheyden V, Devogelaere B, Missiaen L, De Smedt H, Bultynck G, Parys JB. Regulation of inositol 1,4,5-trisphosphate-induced Ca^{2+} release by reversible phosphorylation and dephosphorylation. *Biochim Biophys Acta* 2009; **1793**:959–970.
73. Zhang N, Yoon SY, Parys JB, Fissore RA. Effect of M-phase kinase phosphorylations on type 1 inositol 1,4,5-trisphosphate receptor-mediated Ca^{2+} responses in mouse eggs. *Cell Calcium* 2015; **58**:476–488.
74. Malathi K, Kohyama S, Ho M, Soghoian D, Li X, Silane M, Berenstein A, Jayaraman T. Inositol 1,4,5-trisphosphate receptor (type 1) phosphorylation and modulation by Cdc2. *J Cell Biochem* 2003; **90**:1186–1196.

75. Manosalva I, Gonzalez A. Aging alters histone H4 acetylation and CDC2A in mouse germinal vesicle stage oocytes. *Biol Reprod* 2009; **81**:1164–1171.
76. Tarin JJ, Gomez-Piquer V, Pertusa JF, Hermenegildo C, Cano A. Association of female aging with decreased parthenogenetic activation, raised MPF, and MAPKs activities and reduced levels of glutathione S-transferases activity and thiols in mouse oocytes. *Mol Reprod Dev* 2004; **69**:402–410.
77. Chernorudskiy AL, Zito E. Regulation of calcium homeostasis by ER redox: a close-up of the ER/mitochondria connection. *J Mol Biol* 2017; **429**:620–632.
78. Tatone C, Di Emidio G, Barbaro R, Vento M, Ciriminna R, Artini PG. Effects of reproductive aging and postovulatory aging on themaintenance of biological competence after oocyte vitrification: insights from the mouse model. *Theriogenology* 2011; **76**:864–873.
79. Yamada-Fukunaga T, Yamada M, Hamatani T, Chikazawa N, Ogawa S, Akutsu H, Miura T, Miyado K, Tarín JJ, Kuji N, Umezawa A, Yoshimura Y. Age-associated telomere shortening in mouse oocytes. *Reprod Biol Endocrinol* 2013; **11**:108.
80. Mihalas BP, De Iuliis GN, Redgrove KA, McLaughlin EA, Nixon B. The lipid peroxidation product 4-hydroxynonenal contributes to oxidative stress-mediated deterioration of the aging oocyte. *Sci Rep* 2017; **7**:6247.
81. Pasquariello R, Ermisch AF, Silva E, McCormick S, Logsdon D, Barfield JP, Schoolcraft WB, Krisher RL. Alterations in oocyte mitochondrial number and function are related to spindle defects and occur with maternal aging in mice and humans. *Biol Reprod* 2019; **100**:971–981.
82. Higo T, Hattori M, Nakamura T, Natsume T, Michikawa T, Mikoshiba K. Subtype-specific and ER lumenal environment-dependent regulation of inositol 1,4,5-trisphosphate receptor type 1 by ERp44. *Cell* 2005; **120**:85–98.
83. Dumollard R, Duchen M, Sardet C. Calcium signals and mitochondria at fertilisation. *Semin Cell Dev Biol* 2006; **17**:314–323.
84. Marchi S, Patergnani S, Missiroli S, Morciano G, Rimessi A, Wieckowski MR, Giorgi C, Pinton P. Mitochondrial and endoplasmic reticulum calcium homeostasis and cell death. *Cell Calcium* 2018; **69**:62–72.
85. Kushnir VA, Ludaway T, Russ RB, Fields EJ, Koczor C, Lewis W. Reproductive aging is associated with decreased mitochondrial abundance and altered structurein murine oocytes. *J Assist Reprod Genet* 2012; **29**:637–642.
86. Ben-Meir A, Burstein E, Borrego-Alvarez A, Chong J, Wong E, Yavorska T, Naranian T, Chi M, Wang Y, Bentov Y, Alexis J, Meriano J et al. Coenzyme Q10 restores oocyte mitochondrial function and fertility during reproductive aging. *Aging Cell* 2015; **14**:887–895.
87. Wilding M, Di Matteo L, Dale B. The maternal age effect: a hypothesis based on oxidative phosphorylation. *Zygote* 2005; **13**: 317–323.
88. Kujjo LL, Perez GI. Ceramide and mitochondrial function in aging oocytes: joggling a new hypothesis and old players. *Reproduction* 2012; **143**:1–10.
89. Seli E, Wang T, Horvath TL. Mitochondrial unfolded protein response: a stress response with implications for fertility and reproductive aging. *Fertil Steril* 2019; **111**:197–204.